Journal of Power Sources, 7 (1981/82) 165 - 180

ALKALINE ELECTROLYTE–LITHIUM MINIATURE PRIMARY BATTERIES*

PAUL RUETSCHI
Leclanché S.A., 1400 Yverdon (Switzerland)
(Received September 8, 1980; in revised form July 21, 1981)

Summary

Alkaline aqueous electrolyte miniature batteries, and nonaqueous electrolyte–lithium miniature batteries are compared with respect to constructional features, energy density, rate capability, self-discharge, reliability, and seals. The criteria for valid comparison of such data are discussed.

1. Introduction

Progress in reducing the power requirements of electronic circuits has led to an increased demand for smaller and smaller batteries. The present world market for miniature batteries, mostly of the so-called "button cell" type, is estimated to approach 1 billion items per year. Most applications are to pocket calculators, watches and clocks, hearing aids, cameras, telecommunication and military equipment, instruments, entertainment articles and toys.

Alkaline electrolyte battery systems such as HgO–Zn, Ag_2O–Zn, AgO–Zn, MnO_2–Zn, and air–Zn still dominate the field, but *lithium battery systems* of a bewildering number of types, such as MnO_2–Li, CF_x–Li, Ag_2CrO_4–Li, CuO–Li, Bi_2O_3–Li, Pb_3O_4–Li, $Bi_2Pb_2O_5$–Li, Bi_2CuO_4–Li, TiO_2–Li, V_2O_5–Li, FeS–Li, FeS_2–Li, CuS–Li, I_2(PVP)–Li, SO_2–Li, $SOCl_2$–Li, SO_2Cl_2–Li — to name some of the systems which have received particular attention recently — are developing rapidly and might with time, gain an important part of the button cell market.

Definition of "Miniature Batteries"

As batteries get smaller, at what point do they become "miniature batteries"? One pragmatic, although rather ambiguous criterion is that

*Based on a paper presented at the "Symposium on Miniature Cells", organised by the International Electrochemical Society, Venice, 22 - 26 September, 1980.

relating to their marking or labelling requirements. The International Electrotechnical Commission (IEC) has standardized internationally certain marking requirements. IEC publication 86-1 recommends that each battery should be marked with the following information: designation (electrochemical system and type number), date of manufacture, polarity, nominal voltage, name or trademark of the manufacturer or supplier. As the batteries become so small that it is impossible to provide thereon the complete information, they become "small batteries". Part of the required marking may then be given on the packing, instead of on the battery.

The IEC list of such "small batteries" is growing very rapidly. To date it pertains entirely to *round cells*, of the so-called "button type", *with a height of less than 20 mm*.

The smallest button cells made up to now for electronic watches have a diameter of 6.8 mm and a height of 1.1 mm. The smallest hearing-aid battery in use has a diameter of 5.6 mm and a height of 3.2 mm. Table 1 shows a list of individual cell diameters and cell heights, internationally standardised, or considered for international standardisation, by the IEC. For each diameter given in this list, cells with different heights may exist, and *vice versa*; for each cell height cells of different diameters may exist, as selected from the list.

TABLE 1

Dimensions of miniature watch batteries

Diameter (mm)	Height (mm)
11.6	5.4
9.5	4.2
7.9	3.6
6.8	3.1
	2.6
	2.1
	1.6
	1.1

Construction features

The conventional grommet-sealed button cell construction, Figs. 1 and 2, used for many years for alkaline electrolyte cells [1 - 4], has been adopted in many lithium miniature batteries, such as MnO_2–Li [5, 6], CF_x–Li [7 - 10], CuO–Li [11 - 13], Bi_2O_3–Li, Pb_3O_4–Li, $Bi_2Pb_2O_5$–Li and Bi_2CuO_4–Li [14], FeS–Li and FeS_2–Li [15, 16], Ag_2CrO_4–Li [17, 18], CuS–Li [19, 20], using a liquid organic electrolyte.

The positive electrode, in the form of a flat pellet, is usually housed in a steel can, which also forms the positive terminal. The lithium sheet electrode

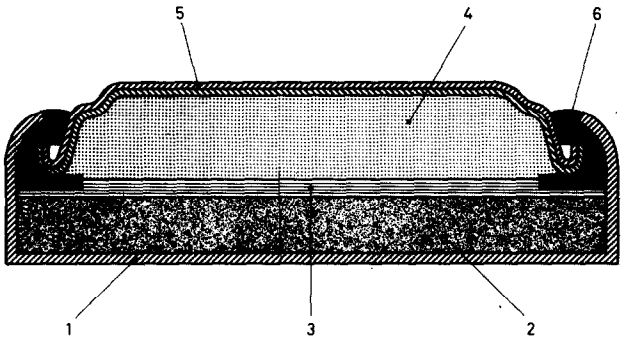

Fig. 1. Cross-section of conventional button cell — 1, can; 2, positive electrode; 3, separator; 4, negative electrode; 5, cover; 6, grommet. (From ref. 2.)

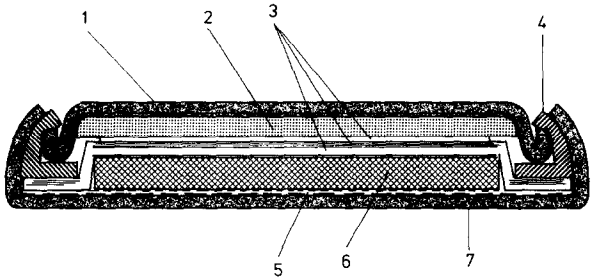

Fig. 2. Very thin button cell — 1, cover; 2, negative electrode; 3, separator layers; 4, grommet; 5, contact member; 6, positive electrode; 7, can. (From ref. 3.)

is pressed onto a nickel or stainless steel screen or expanded metal, welded to the cover, which forms the negative terminal. A grommet is tightly clamped between can and cover by means of crimp-sealing the cell. A crimp seal has also been tried on a solid electrolyte I_2(PVP)–Li cell [21].

However, most lithium miniature cells of the solid electrolyte type, I_2(PVP)–Li [22, 23], and certainly all cells with liquid (or pressurized gas) depolarizer, SO_2–Li, $SOCl_2$–Li, SO_2Cl_2–Li [24] must be constructed with hermetic glass-to-metal feed-throughs, such as are illustrated, for example, in Fig. 3 [25]. Miniature cells with cylindrical electrode configuration, as shown in Fig. 4, have also been constructed [26]. In these cells, the positive electrode has the shape of a tube and lines the inside cylindrical wall of the can, while the rod-shaped negative electrode is centrally located and is surrounded by a separator tube.

2. Performance

Energy density

For very small electrochemical power sources, only the *volumetric energy density* (W h/cm^3), but not the specific energy per unit weight

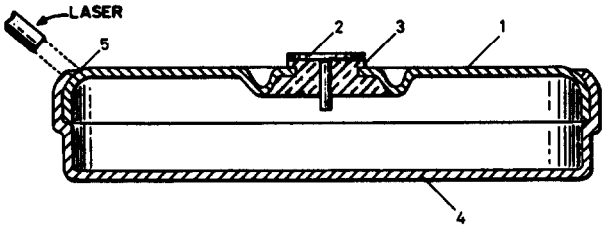

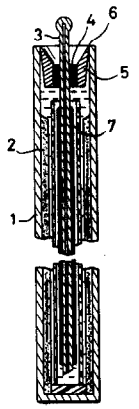

Fig. 3 (left). Button cell with glass-to-metal feed through, according to ref. 25. 1, cover; 2, feed through terminal; 3, glass-to-metal seal; 4, can; 5, laser weld.

Fig. 4 (right). Cylindrical miniature cell with glass-to-metal feed through, according to ref. 26. 1, can; 2, positive electrode; 3, filling tube and negative electrode terminal; 4, glass-to-metal seal; 5, metal cover; 6, weld; 7, lithium electrode.

(W h/g), is usually of interest. The volumetric energy density decreases with cell volume, since the percentage of "dead volume" for containers and seals becomes increasingly significant for smaller cells. This relation is illustrated for commercial HgO–Zn, Ag_2O–Zn and MnO_2–Li cells in Fig. 5.

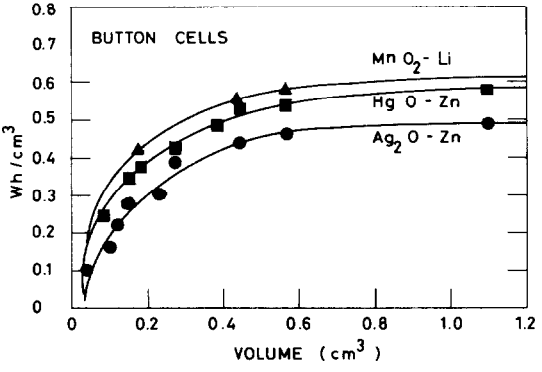

Fig. 5. Energy density (W h/cm^3) of Ag_2O–Zn, HgO–Zn and MnO_2–Li miniature cells, as a function of cell volume.

The volumetric energy density is also a function of the rate of discharge. At high rates, the energy density is reduced, due to electrode polarisation and mass transfer limitations, leading to decreased active material utilisation. At very low discharge rates, on the other hand, the energy density decreases because of self-discharge effects. Figure 6 demonstrates this fact schematically for a normal (low impedance) HgO–Zn cell (curve A) and a long-life (high impedance) cell (curve B), the latter being equipped with a

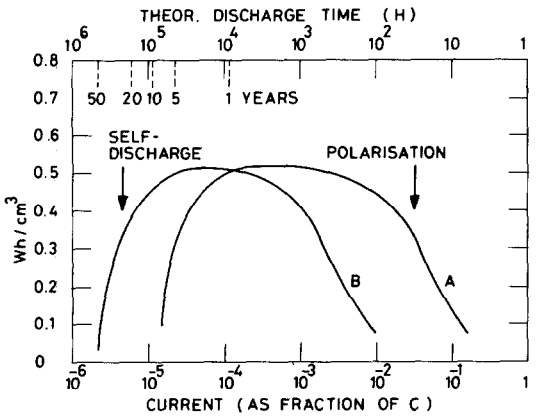

Fig. 6. Energy density (W h/cm^3) of HgO–Zn miniature cells as a function of discharge rate, expressed as fraction of capacity, *C*. Curve A: standard high-rate cell. Curve B: special long-life, low-rate cell.

"current-focusing membrane" and containing a "water-starved" electrolyte, as described below in the section on self-discharge.

When comparing energy densities of different electrochemical systems one must therefore use data for cells of identical volume and of identical discharge rates. Tables 2 and 3 list maximum practical energy densities realized with button cells of 11.6 mm dia. and 4.2 mm height (volume ~0.5 cm^3) at a discharge rate of 5 - 10 μA. (ref. 27 as well as our own measurements.)

TABLE 2

Practical energy density of miniature alkaline button cells (Volume ~0.5 cm^3, discharge rate ~10^{-4}, 20 °C.)

System	Mid-life voltage (V)	Energy density (W h/cm^3)
HgO–Cd	0.90	0.17
MnO_2–Zn	1.30	0.23
NiOOH–Zn	1.55	0.23
Ag_2O–Zn	1.55	0.45
CuO–Zn	0.90	0.50
HgO–Zn	1.35	0.53
AgO–Zn	1.55	0.60
Air–Zn	1.25	0.95

Of the different lithium battery systems, MnO_2–Li miniature button cells are at present the most widely used commercially. Their performance is compared with that of HgO–Zn and Ag_2O–Zn cells in Fig. 7.

TABLE 3

Practical energy density of miniature lithium button cells (Volume ~0.5 cm^3, discharge rate ~10^{-4} C, 20 °C.)

System	Mid-life voltage (V)	Energy density (W h/cm^3)
TiO_2–Li	1.4	0.30
CuS–Li	1.8	0.40
I_2–Li	2.8	0.40
FeS_2–Li	1.6	0.45
CuO–Li	1.4	0.50
CF_x–Li	2.6	0.50
Ag_2CrO_4–Li	3.0	0.50
MnO_2–Li	2.8	0.55
$SOCl_2$–Li	3.5	0.60

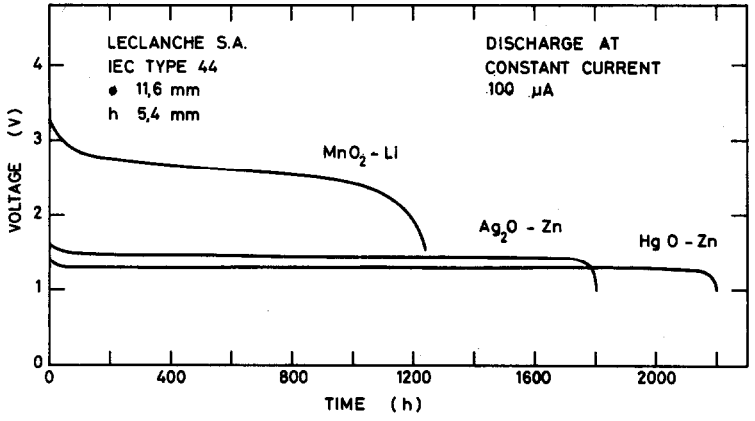

Fig. 7. Comparison of discharge curves of MnO_2–Li, Ag_2O–Zn and HgO–Zn cells of the R44 size (dia. 11.6 mm, height 5.4 mm).

High-rate performance (rate capability, as related to internal impedance)

In most applications today, only very small current drains are required, and service life extends over many months or years, as for instance in calculators, watches, light intensity meters, etc. However, a high-rate (pulse) capability is necessary for watches with LED display. Sustained high-rate discharge capability has to be dealt with in a few special cases only, mostly military, where a low impedance is required also at low temperature. Rate capability can be evaluated by means of transient impedance measurements during discharge, using d.c. current or voltage step methods, or a.c. techniques. Cell impedance of alkaline electrolyte cells usually stays fairly constant throughout discharge, while certain lithium cells, in particular those of the I_2(PVP)–Li solid electrolyte type, show a steady rise [28, 29]. A

schematic comparison of the internal resistance behaviour of Ag_2O–Zn (low drain), HgO–Zn, MnO_2–Li and I_2(PVP)–Li button cells of 11.6 mm dia. and 2.1 mm height is shown in Fig. 8. Internal impedance is, of course, strongly temperature dependent (Fig. 9).

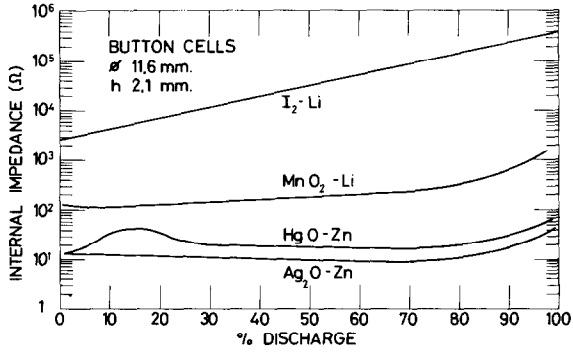

Fig. 8. Increase of internal resistance (impedance) of different button cells as a function of state of discharge. (Discharge rate 10^{-4} C.)

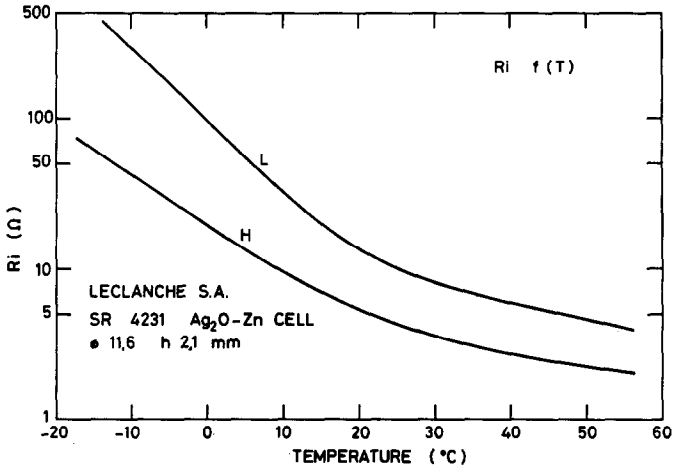

Fig. 9. Internal resistance (impedance) of Ag_2O–Zn button cells, dia. 11.6 mm, height 2.1 mm, as a function of temperature. Curve H: high-rate cells (KOH electrolyte); curve L: low-rate cells (NaOH electrolyte).

Rate capability depends on electrolyte and electrode conductivity, electrode porosity, geometric electrode surface, distance between electrodes, separator porosity, and contact resistance between terminal caps and electrodes, and between conducting material and active material in the positive electrode. Rate capability of both lithium and alkaline electrolyte button cells, can sometimes be improved by placing conducting porous metallic layers or metal screens on top of the positive electrode [30, 31], Figs. 10

and 11. This is particularly the case for positive electrode mixes of low electronic conductivity.

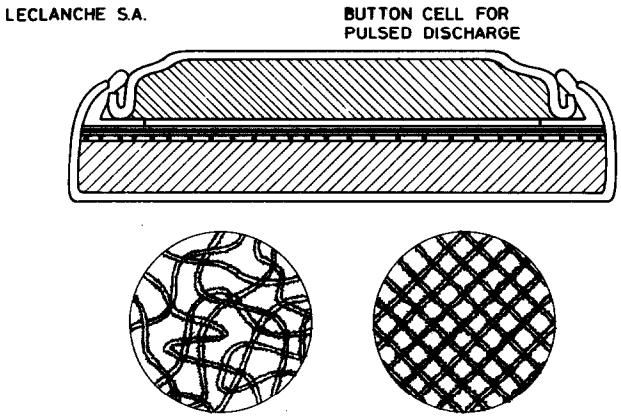

Fig. 10. Button cells for pulse discharge, equipped with graphite coated metallic conducting screen.

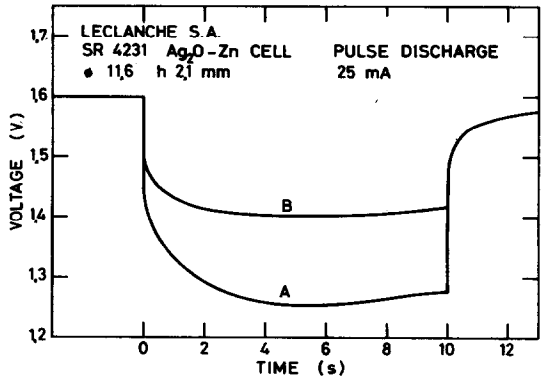

Fig. 11. Pulse discharge behaviour of button cells. Curve A: cell without conducting screen; curve B: cell with conducting screen according to Fig. 10.

As demonstrated in Table 4, lithium batteries can be grouped conveniently into three classes showing widely different rate capabilities:

Class I: cells with liquid (or pressurized gas) depolarizer; Class II: organic electrolyte cells with solid oxide or salt depolarizer; Class III: solid electrolyte type cells.

Internal impedance tends to increase after extended storage periods, especially at elevated temperatures. This loss of rate capability is particularly pronounced with certain lithium cells, as for instance those of the $SOCl_2$–Li type, where a passivating layer on the anode leads to a "voltage delay" phenomenon [32, 33].

TABLE 4

Lithium batteries

Class	Electrolyte	Positive electrode material	Current density mA/cm^2
I	$LiAlCl_4$ in SO_2, $SOCl_2$ or SO_2Cl_2	Liquid or pressurised gas SO_2, $SOCl_2$ or SO_2Cl_2	10^{-3} - 10^{-1}
II	$LiClO_4$ or $LiAlCl_4$ in org. solvent. example: propylene carbonate, γ-butyrolactone dimethoxyethane etc.	Solid oxide or salt MnO_2 CuO Ag_2CrO_4 FeS_2CF_x	10^{-5} - 10^{-3}
III	LiI Solid electrolyte	I_2–poly(2-vinyl)pyridine	10^{-7} - 10^{-5}

Self-discharge

In alkaline electrolyte cells with zinc anodes, major cell-internal self-discharge reactions are oxidation of zinc, by reaction with water, under evolution of hydrogen: $Zn + H_2O \rightarrow ZnO + H_2$, and oxidation of Zn due to dissolved positive active material; in the case of HgO–Zn cells, for instance: $Zn + HgO$ (diss.) $\rightarrow ZnO + Hg$. The two reactions may be coupled together in that H_2 evolution is higher in partly discharged Zn electrodes due to local variations of ZnO_4^{2-} and OH^- concentrations [34]. Storage at elevated temperature is a suitable means of studying self-discharge processes in an accelerated manner. Data relating to the diffusion of dissolved HgO in KOH at 75 °C are shown in Fig. 12. Solubility values were estimated by means of a

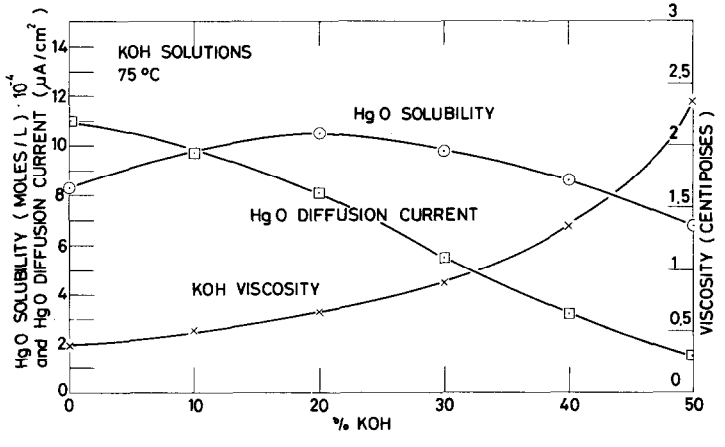

Fig. 12. HgO solubility, HgO diffusion current and KOH viscosity as a function of KOH concentration at 75 °C.

procedure described earlier [35]. HgO diffusion towards the anode, as expressed in terms of a self-discharge current ($\mu A/cm^2$ of separator surface), was measured experimentally by Hg content determination of the anodes in HgO–Cd button cells.

The relative importance of self-discharge due to diffusion of dissolved positive active material depends on cell design, in particular on the ratio between separator interface (diffusion interface) and cell capacity. For a diffusion interface of 1 cm^2, self-discharge, expressed as per cent. capacity loss per year, increases with decreasing capacity, *i.e.*, at a given cell diameter, for instance of 11.6 mm, with decreasing cell height. This is illustrated in Figs. 13 and 14.

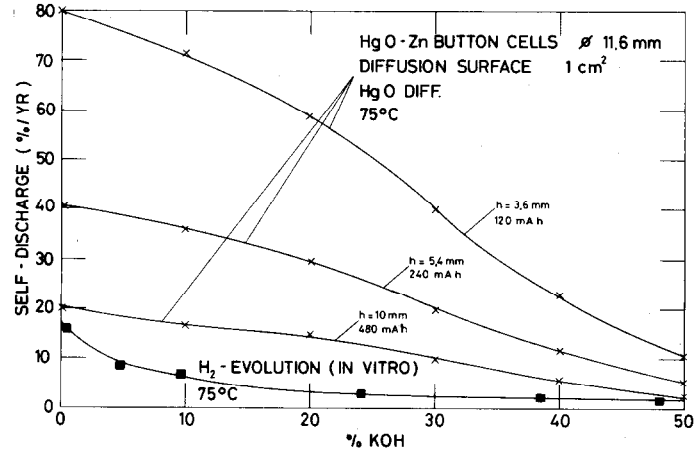

Fig. 13. Part of self-discharge due to HgO diffusion in HgO–Zn button cells of 11.6 mm dia., as a function of KOH concentration. Parameter: cell capacity (or cell height). Also shown is the theoretical self-discharge, due to $Zn + H_2O \rightarrow ZnO + H_2$, calculated from H_2 evolution of Zn powder *in vitro*.

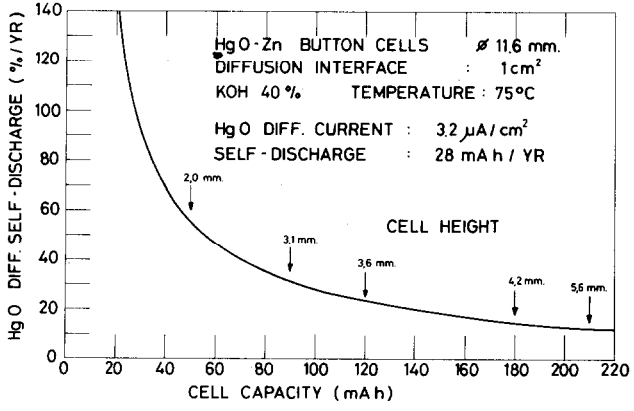

Fig. 14. Part of self-discharge due to HgO diffusion in HgO–Zn cells of 11.6 mm dia., as a function of cell height.

Diffusion of dissolved positive active material towards the negative electrode may be decreased by using less pervious separators, or through obturation of the diffusive flux by means of filter electrodes or focusing membranes [4]. This latter approach is illustrated in Fig. 15. The positive electrode is covered with an inert, very thin membrane, which has been punctured in the center. The entire electrolytic current flow must pass through the small hole in the membrane, but diffusion of dissolved positive active material is thereby drastically hindered. Figure 16 shows the capacity loss of comparative cells at 75 °C, with and without a current focusing membrane. The initial linear decrease of capacity of the cell with a current focusing membrane represents a self-discharge rate of 23%/year at 75 °C.

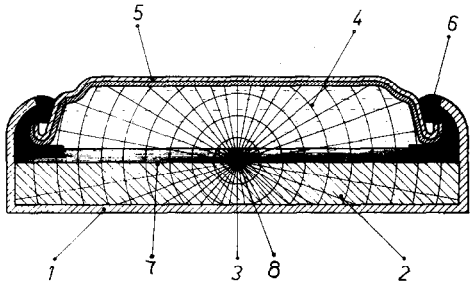

Fig. 15. Schematic representation of current flow in a cell with "focusing membrane" (ref. 4). 1, can; 2, positive electrode; 3, separators; 4, negative electrode; 5, bimetallic cover; 6, sealing grommet; 7, electrolyte-impervious membrane; 8, current focusing aperture.

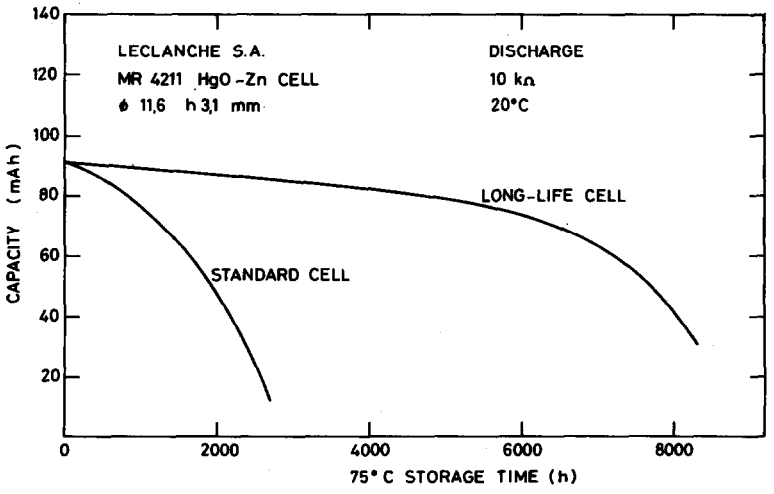

Fig. 16. Capacity loss during storage at 75 °C for cells with (long-life) and without (standard) "focusing membrane".

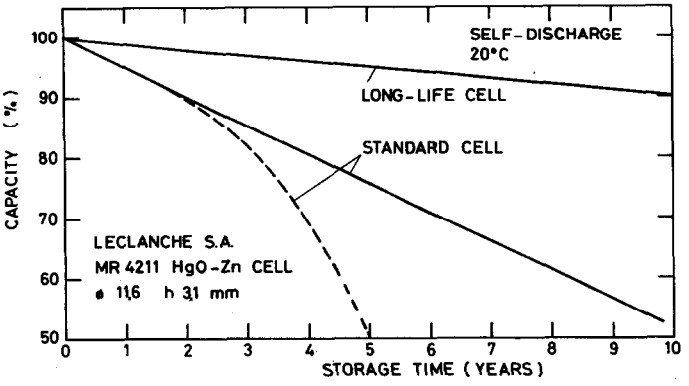

Fig. 17. Projected shelf life at 20 °C of cells with (long life) and without (standard) "focusing membrane".

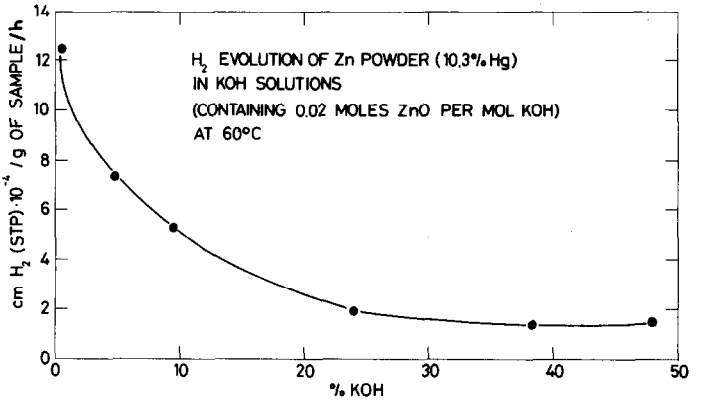

Fig. 18. Hydrogen evolution of amalgamated zinc powder (10.3% Hg) as a function of KOH concentration at 60 °C. Hydrogen volume is expressed in STP cm^3 (0 °C and 760 mmHg).

Projected shelf life at 20 °C for such cells, with and without a current focusing membrane, is illustrated in Fig. 17. Self-discharge may also be decreased by using highly concentrated electrolytes in which the solubility of the active material is decreased and diffusion is slowed down by high viscosity, as demonstrated in Fig. 12. By the same means, self-discharge due to H_2 evolution is also decreased. Figure 18 shows gas evolution of amalgamated Zn powder as a function of KOH concentration at 60 °C. These measurements were carried out with extreme precautions in regard to impurity effects, which have led to earlier erroneous results. Gas evolution of well amalgamated Zn powder (10.3% Hg) *in vitro* is quite low and leads to a calculated self-discharge of less than 3% per year at 75 °C in highly concentrated KOH (Fig. 13). However, under actual cell conditions, H_2 evolution is accelerated due to the presence of the contact surface to the Zn powder

(usually amalgamated copper), the presence of impurity particles stemming from separators and positive electrodes, and the non-homogeneous discharge of the zinc electrode resulting from HgO diffusion. These effects render H_2 evolution in actual cells more than an order of magnitude higher than H_2 evolution *in vitro* [4]. For this reason, H_2 evolution is the dominant self-discharge reaction in alkaline aqueous electrolyte cells.

The described means to lower self-discharge are protected by patent applications. Reduction of self-discharge by these means is generally at the cost of increased cell impedance, Fig. 6. As the maximum tolerable cell impedance is usually well defined, self-discharge, accordingly, can be tailored and minimized to the maximum possible degree for each application.

Claims that lithium cells will in all cases have much lower self-discharge rates than alkaline electrolyte cells should be open to correction. In fact, self-discharge rates of alkaline cells of the special "long-life" type may be lowered to below 1% per year at 20 °C [4], and could thus probably be as low, or lower, than that of the best lithium cells [29, 36 - 39]. Cell-external self-discharge, due to the "oxygen cycle" and "electrolysis" in moisture films present on the external cell walls, can contribute very significantly to total self-discharge [34, 35].

The self-discharge of HgO–Zn alkaline electrolyte, and grommet sealed MnO_2–Li organic electrolyte miniature batteries is compared in Figs. 19 and 20. Lithium cells with grommet seals probably lose electrolyte solvent by evaporation through the grommet during high-temperature storage. The data of Figs. 19 and 20 have been compiled from our own measurements and data published recently by Krüger [40].

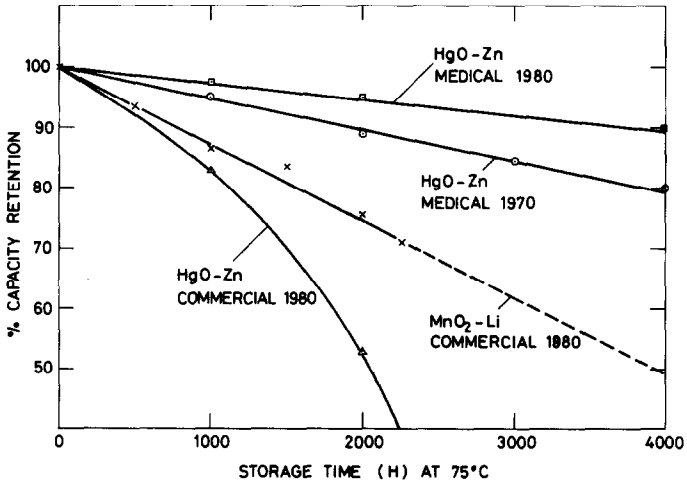

Fig. 19. Self-discharge during storage at 75 °C of HgO–Zn and MnO_2–Li button cells. HgO–Zn (commercial) refers to commercial grade watch cells of 11.6 mm dia. and 3.1 mm height; HgO–Zn (medical) refers to medical grade cells of 15.8 mm dia. and 16.4 mm height. MnO_2–Li (commercial) refers to a flat button cell, 20 mm dia., 1.6 mm height.

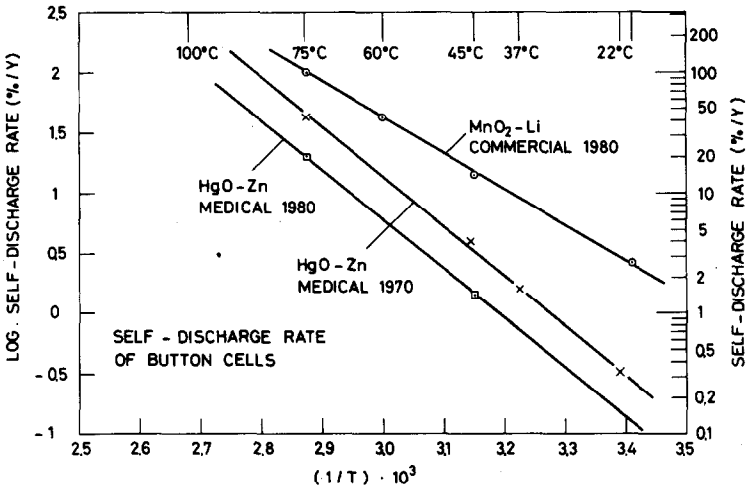

Fig. 20. Self-discharge of medical grade HgO–Zn cells (dia. 15.8 mm, height 16.4 mm) and commercial grade MnO_2–Li cells (dia. 20 mm, height 1.6 mm).

Reliability and seals

Early versions of alkaline mercuric oxide–zinc cells exhibited a high failure rate during low-rate discharge due to internal shorts, caused by migrating mercury droplets. Improved cell designs have corrected this problem. When careful quality control procedures are applied, alkaline electrolyte cells of extremely high reliability may be built, equaling that of lithium cells [41] (failure rates of 10^{-7} - 10^{-8}/h).

A major concern with alkaline miniature cells has been seal reliability, although much progress has been made in recent years in this area [42], especially through the use of special grommet treatments [43 - 45]. Alkaline electrolytes have a higher creep-tendency than organic electrolytes, such as $LiClO_4$ in propylene carbonate–dimethoxyethane, as used, *e.g.*, in MnO_2–Li, CF_x–Li, CuO–Li, Bi_2O_3–Li or FeS_2–Li cells. However, hermetic glass-to-metal seals could possibly still improve seal reliability and storage characteristics for these organic electrolyte systems [40, 46]. Hermetic ceramic-to-metal seals are also of interest for long-life alkaline cells [47, 48]. Solid electrolyte–lithium cells (I_2(PVP)–Li) and, in particular, liquid depolariser–lithium cells (SO_2–Li, $SOCl_2$–Li, SO_2Cl_2–Li) must make use of hermetic glass-to-metal or ceramic seals because of the very corrosive nature of the depolarizer materials, rendering long-term reliable sealing quite difficult [49, 50].

3. Conclusions

Lithium button cells are rapidly emerging as a new generation of miniature power sources. Construction features of organic electrolyte–lithium button cells resemble those of their alkaline electrolyte counterparts.

In comparing energy densities of various miniature battery systems one must take into account the influence of cell size and discharge rate.

Rate capability varies widely, depending on internal construction. Lithium cells may be grouped into 3 classes: (i) liquid or pressurized gas depolarizer cells; (ii) organic electrolyte–solid oxide depolarizer cells; (iii) solid electrolyte cells.

Self discharge of special long-life alkaline electrolyte cells may be as low as, or lower than, that of lithium cells.

Seal reliability has been greatly improved in recent years for alkaline electrolyte cells (*e.g.*, by using special grommet treatments). Lithium cells with organic electrolytes appear to present less problems in respect of leakage than do alkaline electrolyte cells. Glass-to-metal and ceramic-to-metal seals are being used for solid electrolyte (I_2(PVP)–Li) and liquid or pressurized gas depolarizer (*e.g.*, $SOCl_2$–Li) lithium cells, and are also of interest for organic electrolyte–lithium cells, as well as for aqueous alkaline electrolyte cells.

References

1 S. Rubens, *U.S. Patent 2,422,045*, June 10, 1947.
2 P. Ruetschi, in D. H. Collins (ed.), *Power Sources, 4*, Oriel Press, Newcastle upon Tyne, 1973, p. 381.
3 P. Ruetschi, *U.S. Patent 4,209,574*, June 24, 1980.
4 P. Ruetschi, *J. Electrochem. Soc., 127* (1980) 1667.
5 H. Ikeda, M. Hara and H. Tamura, *Prog. Batteries Solar Cells, 1* (1978) 19.
6 H. Ikeda, M. Hara and S. Narukawa, *Proc. 28th Power Sources Symp.*, The Electrochemical Society, Princeton, NJ, 1980, p. 210.
7 M. Fukuda and T. Iijima, *Prog. Batteries Solar Cells, 1* (1978) 26.
8 J. Watanabe, E. Kawakubo, I. Shinagawa and Y. Kajikawa, *Prog. Batteries Solar Cells, 3* (1980) 74.
9 A. Morita, T. Iijima, T. Fujii and H. Ogawa, *J. Power Sources, 5* (1980) 111.
10 R. Chireau, *Proc. 28th Power Sources Symp.*, The Electrochemical Society, Princeton, NJ, 1978, p. 203.
11 H. Ogawa, T. Iijima, A. Morita and J. Nishimura, *Prog. Batteries Solar Cells, 3* (1980) 93.
12 T. Iijima, Y. Toyoguchi, J. Nishimura and H. Ogawa, *J. Power Sources, 5* (1980) 99.
13 Y. LeRoy, *Microtechniques*, ECI, Paris, Hors Série, April 1981, p. 39.
14 M. Broussely, Y. Jumel and J. P. Gabano, *J. Power Sources, 5* (1980) 83. *Prog. Batteries Solar Cells, 2* (1979) 84. In H. V. Venkatasetty (ed.), *Proc. Symp. on Lithium Batteries*, The Electrochemical Society, Princeton, NJ, 1981, p. 340.
15 Y. Uetani, K. Yokohama and O. Okamoto, *J. Power Sources, 5* (1980) 89.
16 J. C. Nardi, M. B. Clark and W. P. Evans, *Microtechniques*, ECI, Paris, Hors Série, April 1981, p. 48.
17 G. Gerbier, G. Lehmann and P. Lenfant, *Prog. Batteries Solar Cells, 1* (1978) 32.
18 J. P. Arzur, *Microtechniques*, ECI, Paris, Hors Série, April 1981, p. 31.
19 B. C. Bergum, A. M. Bredland and T. Messing, *Prog. Batteries Solar Cells, 3* (1980) 90.
20 A. J. Cuesta and D. D. Bump, in B. B. Owens and N. Margalit (eds.), *Symp. on Power Sources for Biomedical Implantable Applications and Ambient Temperature Lithium Batteries*, The Electrochemical Society, Princeton, NJ, 1980, p. 95.
21 T. Sotomura, M. Nakai, S. Sekido and J. Watanabe, *Prog. Batteries Solar Cells, 2* (1979) 44.

22 A. Schneider, D. Harney and M. Harney, *J. Power Sources, 5* (1980) 15.
23 E. S. Hatch, A. Schneider and J. L. Stegmann, *Microtechniques,* ECI, Paris, Hors Série, April 1981, p. 45.
24 N. Marincic and J. Epstein, *Prog. Batteries Solar Cells, 3* (1980) 84.
25 J. J. Decker and D. J. Kantner, *UK Patent Application G.B. 2,020,888 A,* May 10, 1979.
26 A. N. Dey, *U.S. Pat. 4,053,692,* Oct. 11, 1977.
27 S. A. Megahed and D. C. Davig, *Adv. Battery Technol., 16* (2/3) (1980) 54. R. M. Rasmussen, *Microtechniques,* ECI, Paris, Hors Série, April, 1981, p. 19.
28 A. A. Schneider, S. E. Snyder, T. DeVan, M. J. Harney and D. E. Harney, in B. B. Owens and N. Margalit (eds.), *Proc. Symp. Power Sources for Biomedical Implantable Applications and Ambient Temperature Lithium Batteries,* The Electrochemical Society, Princeton, NJ, 1980, p. 144.
29 B. B. Owens and D. F. Untereker, in J. Thompson (ed.), *Power Sources 7,* Academic Press, London, 1979, p. 647.
30 R. A. Langan, N. J. Smilanich and A. Kozawa, *U.S. Pat.4,015,055,* March 29, 1977.
31 P. Ruetschi, *Brit. Pat. 1,558,157,* March 30, 1977.
32 A. Leef and A. Gilmour, *J. Appl. Electrochem., 9* (1979) 663.
33 J. P. Gabano and G. Gelin, in J. Thompson (ed.), *Power Sources 8,* Academic Press, London, New York, 1981, in press.
34 P. Ruetschi, in J. Thompson (ed.), *Power Sources 7,* Academic Press, London, 1979, p. 533.
35 P. Ruetschi, in B. B. Owens and N. Margalit (eds.), *Symp. Power Sources for Biomedical Implantable Applications and Ambient Temperature Lithium Batteries,* The Electrochemical Society, Princeton, NJ, 1980, p. 34.
36 B. Babai and Y. Gal, in B. B. Owens and N. Margalit (eds.), *Symp. Power Sources for Biomedical Implantable Applications and Ambient Temperature Lithium Cells,* The Electrochemical Society, Princeton, NJ, 1980, p. 536.
37 W. D. Helgeson and K. E. Fester, in B. B. Owens and N. Margalit (eds.), *Symp. Power Sources for Biomedical Implantable Applications and Ambient Temperature Lithium Cells,* The Electrochemical Society, Princeton, NJ, 1980, p. 154.
38 C. C. Liang and C. F. Holmes, *J. Power Sources, 5* (1980) 3. *Prog. Batteries Solar Cells, 2* (1979) 50.
39 D. Linden and B. McDonald, *J. Power Sources, 5* (1980) 35.
40 D. F. Krüger, *Microtechniques,* ECI, Paris, Hors Série, April 1981, p. 27.
41 G. Gerbier, G. Lehmann, P. Lenfant and J. P. Rivault, in D. H. Collins (ed.), *Power Sources 6,* Academic Press, London, 1977, p. 483.
42 L. M. Baugh, J. A. Cook and F. L. Tye, in J. Thompson (ed.), *Power Sources 7,* Academic Press, London, 1979, p. 519.
43 K. Sugimoto, T. Sakai and N. Kamata, *Microtechniques,* ECI, Paris, Hors Série, April 1981, p. 68.
44 Y. Uetani, S. Shimizu and K. Kajita, *Microtechniques,* ECI, Paris, Hors Série, April 1981, p. 64. K. Kajita, A. Shimuzu and Y. Uetani, *Prog. Batteries Solar Cells, 3* (1980) 99.
45 A. Shimuzu, *Prog. Batteries Solar Cells, 1* (1978) 44.
46 H. Ikeda, S. Narukawa, H. Inokuchi and S. Nakaido, *Microtechniques,* ECI, Paris, Hors Série, April 1981, p. 35.
47 J. A. Topping and P. Mayer, *U.S. Pat. 4,199,340,* April 22, 1980.
48 M. J. Fairweather and J. A. Topping, *Canadian Pat. 1,000,353,* Nov. 23, 1976.
49 B. Jagid, T. Watson and S. M. Chodosh, in B. B. Owens and N. Margalit (eds.), *Proc. Symp. on Power Sources for Biomedical Implantable Applications and Ambient Temperature Lithium Batteries,* The Electrochemical Society, Princeton, NJ, 1980, p. 615.
50 B. C. Bunker, S. C. Levy, C. J. Leedecke and C. C. Crafts, in J. Thompson (ed.), *Power Sources 8,* Academic Press, London, 1981, in press.